I.M. Daniel · E.E. Gdoutos · Y.D.S. Rajapakse
Editors

Major Accomplishments in Composite Materials and Sandwich Structures

An Anthology of ONR Sponsored Research

2009

Springer

Size Effect on Fracture of Composite and Sandwich Structures

Emmanuel E. Gdoutos and Zdeněk P. Bažant

Abstract The objective of this article is to review the work performed on the scaling and size effect in the failure of composites, foams and laminate–foam sandwiches. These materials exhibit quasibrittle behavior which is characterized by a fracture process zone that is not negligible compared to the characteristic size of the structure. The mean size effect is found to be essentially deterministic, caused by energy release due to stress redistribution. The chapter consists of six sections: After introduction, the second section deals with the size effect on the nominal strength of notched specimens of fiber composite laminates under tension. In the third section, the size effect of fiber–composite laminates on flexural strength is studied. The fourth section studies the effect of structure size on the nominal strength of fiber–polymer composites failing by propagation of a kink band with fiber microbuckling. The fifth section deals with the size effect of fracture of closed-cell polymeric foams. The sixth section analyzes the size effect on the compressive strength of sandwich panels subjected to double eccentric axial load and failing by propagation of a softening fracturing kink band. Finally, the seventh section shows that skin imperfections, considered to be proportional to the first eigenmode of wrinkling, lead to strong size dependence of the nominal strength of sandwich structures failing by skin wrinkling.

1 Introduction

The effect of structure size on its nominal strength is of paramount importance in extrapolating small-scale laboratory tests to full-scale structures. The question of size effect was discussed by Leonardo da Vinci (1452–1519) who ran tests to determine

E.E. Gdoutos
School of Engineering, Democritus University of Thrace, GR-67100 Xanthi, Greece
e-mail: egdoutos@civil.duth.gr

Z.P. Bažant (✉)
Department of Civil Engineering and Material Science, Northwestern University,
Evanston, IL 60208-3109, USA
e-mail: z-bazant@northwestern.edu

I.M. Daniel et al. (eds.), *Major Accomplishments in Composite Materials and Sandwich Structures: An Anthology of ONR Sponsored Research*,

the strength of iron wires [1]. He found an inverse proportionality of the nominal strength to the length of the wire for wires of constant diameter. We quote from an authoritative translation of Leonardo's sketch book [2]: "Observe what the weight was that broke the wire, and in what part the wire broke... Then shorten the wire, at first by half, and see how much more weight it supports; and then make it one quarter of its original length, and so on, making various lengths and noting the weight that breaks each one and the place in which it breaks." This is of course a strong exaggeration of the actual size effect.

The rule of Leonardo was rejected by Galileo in his famous book [3], in which he founded mechanics of materials. Galileo argued that cutting a long cord at various points should not make the remaining part stronger. He pointed out, however, that a size effect is manifested in the fact that large animals have relatively bulkier bones than small ones. Half a century later, Mariotte [4] based on extensive experiments on ropes, paper and tin made the observation that "a long rope and a short rope always support the same weight unless that in a long rope there may happen to be some faulty place in which it will break sooner than in a shorter." He thus initiated the statistical theory of size effect, two and a half centuries before Weibull.

The above studies concern with the structural size effect which is studied in this paper. This differs from the material size effect, which was first systematically studied by Griffith [5, 6], who with his key ideas about the strength of solids laid down the foundation of the present theory of fracture. In experiments performed on cracked circular tubes made of glass, Griffith observed that the maximum tensile stress in the tube was of the magnitude of 344 kip/in.^{2} (2,372 MPa), while the tensile strength of glass was 24.9 kip/in.^{2} (172 MPa). These results led him to raise the following questions (we quote from Ref. [5]) "If the strength of this glass, as ordinarily interpreted, is not a constant, on what does it depend? What is the greatest possible strength, and can this strength be made for technical purpose by appropriate treatment of the material?" From Griffith's experiments it follows that the strength increases as the fiber diameter decreases. The maximum strength of glass was found to be 1,600 kip/in.^{2} (11,000 MPa), which is two orders of magnitude higher than the ordinary strength of glass of 24.9 kip/in.^{2} (172 MPa). Stanton and Batson [7] reported the results of tests conducted on notched-bar specimens at the National Physical Laboratory, Teddington, England, after the First World War. From a series of tests it was obtained that the work of fracture per unit volume was decreased as the specimen dimensions were increased.

Weibull [8] laid down the basic framework of the statistical theory of size effect. The theory applies to structures that fail at the initiation of macroscopic fracture and have at fracture only a small fracture process zone causing negligible stress redistribution. This is the case of brittle materials. It does not apply to quasibrittle materials, such as concrete and mortar made with various cements and admixtures, polymers, rock, ice, fiber or particulate composites, fiber-reinforced concretes, toughened ceramics, bone, biological shells, stiff clays, cemented sands, grouted soils, coal, paper, wood, wood particle board, various refractories, some special tough metallic alloys, filled elastomers, etc., which are characterized by the existence of a large fracture process zone with distributed cracking damage.

Weibull's theory attributing the observed size effect to the randomness of material strength dominated until the early 1980s, when Bažant [9, 10] revisited the size effect on structural strength. The classical theories of solid mechanics including elasticity and plasticity do not account for the size effect; in other words, the nominal strength of a structure is independent of its size. This is acceptable only for very small structures. This property is not valid for materials that, instead of plastic yielding, exhibit softening damage, such as distributed cracking. In that case, a strong, non-statistical size effect may be caused by stress redistribution creating energy release from an elastically unloaded region of material at the flanks of a propagating damage or large cohesive fracture, taking place before the maximum load is reached. When this deterministic size effect occurs, it normally prevails over the size effect due to the statistical distribution of strength, described by the Weibull theory. In order to extrapolate to large sizes from material strength values obtained from laboratory tests of relatively small specimens, the size effect should be well understood.

Bažant laid down the foundation of a new concept with his discovery of a deterministic scaling law based on the release of stored energy due to stable growth of large fractures or large damage zones prior to failure [9, 10]. He derived a simple formula for the size effect law which describes the size effect on nominal strength of structures made of quasibrittle materials, which are characterized by the existence of a sizable fracture process zone at the tip of the macroscopic crack. Quasibrittle materials are brittle materials characterized by a fracture process zone (FPZ) that is not negligible compared to the characteristic size D (or cross-sectional dimension) of the structure. Typically, the size of the FPZ, taken as the material characteristic length l_{ch}, is about 5 to 50 times the maximum inhomogeneity size, and quasibrittle behavior is observed only for $D/l_{ch} \sim 1$ to 1,000. For larger D/l_{ch}, the FPZ can be regarded as a point and then the behavior is brittle, while for $D/l_{ch} < 1$, and approximately for up to about 5, the behavior can be regarded as quasi-plastic. Bažant found that in such materials the size effect is transitional between plasticity (for which there is no size effect) and linear elastic fracture mechanics (for which the size effect is the strongest). The curve of the logarithm of the nominal strength versus the logarithm of the size represents a smooth transition from a horizontal asymptote corresponding to the strength criterion (plastic limit analysis) to an inclined asymptote of slope -0.5, corresponding to linear elastic fracture mechanics. He also formulated the crack band model [11, 12] which realistically approximates by simple finite element analysis the size effect observed on concrete specimens and structures. This model is nowadays almost the only concrete fracture or damage model used in industry and commercial codes (e.g. code DIANA, Rots 1988; code SBETA, Červenka and Pukl 1994; or ATENA). A more general nonlocal approach to strain-softening damage, capable of describing the size effect in quasibrittle materials in a more fundamental and realistic manner was published by Bažant et al. [13], Bažant [14], Pijaudier-Cabot and Bažant [15], Bažant and Pijaudier-Cabot [16], and Bažant and Lin [17, 18]. It is used in commercial code OOFEM and in many research projects.

Carpinteri et al. [19] proposed, on the basis of strictly geometrical arguments, that the difference in fractal characteristics of cracks or microcracks at different scales of

observation is the principal cause of size effect in concrete structures. Carpinteri's theory was subject to extensive criticism by Bažant and Bažant and Yavari [20–22].

This article reviews the work performed by Bažant and coworkers on the scaling and size effect in the failure of advanced composite, foams and sandwich materials. The size effect of the above materials is described in six sections for fiber–composite laminates subjected to tension, compression and flexural loading, to closed-cell polymeric foams and to sandwich panels under eccentric compression and with skin imperfections. Each section includes an introduction, experimental results, the size effect law for the particular problem and conclusions.

2 Size Effect on the Tensile Strength of Notched Fiber–Composite Laminates [23]

2.1 Introduction

Failure of composite materials has been described by conventional failure criteria based on maximum stress, maximum strain, deviatoric strain energy (Tsai-Hill) and tensor polynomial (Tsai-Wu). These criteria are macromechanical and do not account for the various micromechanical failure processes occurring in composites, especially near notches. Damage initiation and development take the form of various interacting failure mechanisms which are sensitive to pre-existing defects and micro-structure (micromechanical) anomalies. The damage processes tend to localize and propagate. Their propagation can be studied by energy release, which accounts for the size effect.

Fracture of laminated composites with stress concentrators has been studied by using linear-elastic fracture mechanics and the local stress distributions near the notch end. The first approach based on linear elastic fracture mechanics was used by Waddoups et al. [24] who proposed a theory based on the generalized concept of the process zone. The actual crack length is extended by the length of the process zone which is taken equal to a damage zone at the crack tip. Cruse [25] calculated the fracture energy of a multidirectional laminate as the sum of fracture energies of the individual plies. An equivalent summation of the squares of the stress intensity factors has also been proposed by Mandell et al. [26], who pointed out that microcracking zones play the same role as plastic flow in metals, relieving the high local stress concentrations and absorbing the energy released due to fracture propagation. These authors indicated that the damage zone at the crack tip in fiber composite laminates consists of matrix cracks parallel to the fibers and local delaminations of the cracked plies. Following the second approach of local stress distribution near the notch end, Whitney and Nuismer [27] proposed two simplified fracture criteria based on the actual stress distribution near the notch, the so-called point stress and average stress criteria.

Daniel [28–32] observed that failure of graphite fiber/epoxy matrix composite laminates involves a combination of several microscopic failure mechanisms, including ply microcracking, delamination, fiber breakage and fiber pullout. He found that there is a critical damage zone at the tip of a notch or at the boundary of a hole, whose size at failure was roughly independent of the notch length. These observations revealed the existence of a characteristic length in composite materials. Daniel introduced an equivalent crack equal to the original crack plus the length of the damage zone and calculated an apparent stress intensity factor which was constant for the range of his data, including mixed mode loading. Daniel used his results to obtain an R-curve (resistance curve), giving the dependence of the apparent stress intensity factor on the crack length.

In this work the size effect law of Bažant is used to predict the size effect on the nominal strength of single and doubled notched specimens of graphite/epoxy composite laminates.

2.2 Experimental

Unidirectional, crossply and quasi-isotropic composite laminates were made of IM7/8551-7A (Hercules) graphite/epoxy unidirectional prepreg. The material was fully characterized by testing $[0_6]$, $[90_8]$, and $[10_6]$ coupons under uniaxial tension. Two sets of specimens were prepared for the fracture tests: crossply of $[0/90_2]_s$ layup, and quasi-isotropic of $[0/\pm 45/90]_s$ layup. Each set consisted of four rectangular specimens of the same thickness but different sizes, geometrically similar in the plane of the laminates, with gage length of $6.4 \times 25, 12.7 \times 51, 25.4 \times 102$, and 50.8×203 mm ($0.25 \times 1.0, 0.50 \times 2.0, 1.00 \times 4.0$ and 2.00×8.0 in.). The size ratios were 1:2:4:8. The thickness of the crossply and the quasi-isotropic specimens was 0.76 mm (0.030 in.) and 1.02 mm (0.040 in.). Two edge notches of length $a = D/16$ were machined in the crossply specimens and a single edge notch of length $a = D/5$ was machined in the quasi-isotropic specimens, where D is the specimen width (Fig. 1). The crack tip radius was 0.1 mm (0.004 in.) in all cases. All specimens were tabbed with 38 mm (1.5 in.) long glass/epoxy plates.

The specimens were subjected to a uniaxial tensile loading in an Instron servohydraulic testing machine at a constant crosshead rate for the double edge notched specimens and under crack opening displacement (COD) control for the single-edge-notched specimens. The crosshead rate was adjusted for the different size specimens so as to achieve roughly the same average strain rate of 0.2%/min. in the gage section. With that rate, the peak load was reached within approximately 10 min in all cases.

Figure 2 shows typical stress–strain curves for the notched crossply specimens of various sizes. Note that for the largest specimen size, these curves are almost linear up to failure, while for the smallest specimen size there is a significant nonlinear segment before the peak stress. This indicates a pronounced brittle behavior for the large specimens and a hardening inelastic behavior and reduced brittleness

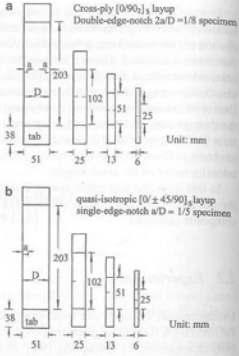

Fig. 1 Geometry of test specimens: (**a**) double-edge notched specimens, (**b**) single-edge notched specimens (units: mm)

(or higher ductility) for the small specimens. The failures of the specimens were catastrophic (dynamic), and occurred shortly after the peak load. Damage consisting of microcracks in layers and delamination between layers before peak load was observed. The nominal strength is defined as the average stress at failure based on the unnotched cross section, $\sigma = P_{max}/hD$ where D is the specimen width (characteristic dimension) and h the laminate thickness.

2.3 *Size Effect*

The approximate size effect law of Bažant [9, 10, 33] is given by

$$\sigma_N = Bf_u(1+\beta)^{-1/2}, \beta = D/D_0 \qquad (1)$$

where

β = relative structure size
$\sigma_N = c_N P/bD$ = nominal strength of structure
P = maximum load
D = characteristic dimension (size) of structure
b = width of structure in the third dimension

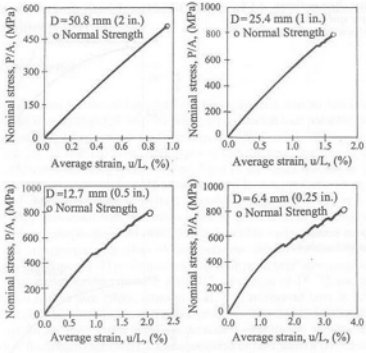

Fig. 2 Typical stress–strain curves of $[0/90_2]_s$ crossply double-edge notched specimens of various sizes, showing increasing nonlinearity with decreasing size

c_N = chosen coefficient introduced for convenience (for example to make σ_N coincide with the maximum stress in the specimen calculated by bending theory)
D_0 = constant depending on both fracture process zone size and specimen geometry
B = constant characterizing the solution according to plastic limit analysis based on the strength concept
f_u = reference strength of the material (laminate), introduced to make constant B dimensionless.

Equation (1) is valid not only for the two-dimensional similarity considered here (h = constant) but also for three-dimensional similarity.

The parameters of the size effect law were determined by regression analysis of experimental data. It was obtained that $D_0 = 30.9$ mm, $Bf_u = 892$ MPa for the crossply specimens, and $D_0 = 77.5$ mm, $Bf_u = 611$ MPa for the quasi-isotropic specimens. The resulting size effect was represented by plotting log (σ_N/Bf_u) versus log (D/D_0) in Figs. 3 and 4 for the two sets of specimens. These size effect plots represent a transition from the strength criterion (plastic limit analysis) characterized by a horizontal asymptote, to an asymptote of slope -0.5, representing linear elastic fracture mechanics (LEFM). The intersection of the two asymptotes corresponds to $D = D_0$, called the transitional size.

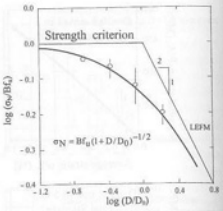

Fig. 3 Size effect measured for crossply specimens with double-edge notches

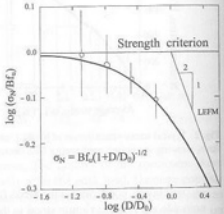

Fig. 4 Quasi-isotropic specimens with single-edge notch

2.4 *Conclusions*

From the results, the following conclusions may be drawn:

1. The nominal strength of composite laminate specimens that are similar and have similar notches or initial traction-free cracks exhibits a significant size effect.
2. The size effect observed agrees with the size effect law proposed by Bažant, according to which the curve of the logarithm of the nominal strength versus the logarithm of the characteristic dimension (size) exhibits a smooth transition from a horizontal asymptote corresponding to the strength criterion (plastic limit analysis) to an inclined asymptote of slope −0.5, corresponding to linear elastic fracture mechanics.
3. Measurements of the size effect on the nominal strength can be used for determining the fracture characteristics of notched fiber composite laminates, including their fracture energy and the effective length of the fracture process zone. From these characteristics, the R-curve can also be calculated.

3 Size Effect on the Flexural Strength of Fiber–Composite Laminates [34]

3.1 *Introduction*

The size effect on the flexural strength of fiber–polymer laminates has been studied by many investigators [35–38]. Wisnom [35] conducted four-point bending tests and pin-ended buckling tests on unidirectional XAS/913 carbon fiber–epoxy specimens with 25, 50, and 100 plies. Both types of tests showed a significant decrease in strength with increasing specimen size. Most of the small specimens failed in tension, while most of the large specimens failed in compression. From the experimental data he obtained a Weibull modulus (shape parameter) $m = 25.4$. Jackson [36] performed tests on beams made of unidirectional, angle-ply, crossply and quasi-isotropic ply-level AS4/3502 carbon fiber–epoxy matrix composites, and found an apparent size effect of the specimen size on the flexural strength. Wisnom and Atkinson [37] performed tests on four-point bend specimens of three-dimensional-scaled unidirectional E glass/913 specimens of 16, 32 and 64 plies, and showed a clear size effect. Johnson et al. [38] performed tests in AS4/3502 graphite–epoxy laminate beams in the four-point bending, and found that the flexural strength of ply-level scaled laminates decreased significantly with the specimen size, while the sublaminate-level scaled specimens did not show a pronounced size effect. The Weibull modulus values for the angle-ply and quasi-isotropic specimens were obtained as 50.0 and 26.7, respectively.

In the present work the size effect on the flexural strength of fiber–polymer composite laminate beams failing at fracture initiation is analyzed by an energetic-statistical size effect law. The size effect is due to stress redistribution engendered by a boundary layer of cracking in structures that fail at the initiation of fracture from a smooth surface, and also by statistics.

3.2 *Size Effect*

For the analysis of the size effect in fiber composite beams under flexural bending the concept of the boundary layer is introduced. The boundary layer develops at the tensile face and has a finite thickness $2D_b$ that is a property of the fiber composite. The laminate cross section is considered homogeneous, so that the elastic bending stress diagram is linear. The laminate is assumed to fail in tension rather than in compression (although compression failure would lead to a similar formula). The average tensile strength of the boundary layer, $f^0{}_r$, which is considered to be a constant, is given by

$$f_r = M_0(D - D_b)/2I \tag{2}$$

where

D = beam depth
M_0 = bending moment
$I = D^3/12$ = moment of inertia of cross section
f^0_r = the average tensile strength of the boundary layer, considered to be constant.

The nominal flexural strength σ_N is defined as the maximum stress in the beam $\sigma_N = f_r = M_0 D/2I$. Therefore,

$$\sigma_N = f_r^0 \left(1 - \frac{D_b}{D}\right)^{-1} \tag{3}$$

The above equation gives negative σ_N for small values of the beam depth D. Thus it is used only for large sizes $D \gg D_b$. This limitation is not surprising because the derivation has been correct only up to the first two terms of the asymptotic series expansion in terms of the powers of $1/D$ [39]. Through a power series expansion in $1/D$ one may check that by making the replacement $(1 - D_b/D)^{-1} \approx (1 + rD_b/D)^{1/r}$ (r being any positive constant signifying a transition slowness parameter), the first two terms of the asymptotic expansion in terms of $1/D$ are not affected while, at the same time, σ_N, becomes positive, finite and monotonically decreasing through the entire range of D. With this replacement, Eq. (3) leads to the size effect formula:

$$\sigma_N = f_r = f_r^0 q(D), \quad q(D) = \left(1 + \frac{rD_b}{D}\right)^{1/r} \tag{4}$$

where $q(D)$ is a positive dimensionless decreasing function of size D having a finite limit for $D \to \infty$.

Equation (4) may be modified as follows:

$$\sigma_N = f_r^0 q\,(D), \quad q(D) = \left(1 + \frac{rD_b}{D + rsD_b}\right)^{1/r} \tag{5}$$

where s is a non-negative constant.

In situations where the Weibull statistical size effect is considered to play a role when the local strength of material elements is random and the minimum of random strength encountered in the structure decreases with the structure size, Bažant and Novak [40, 41] derived the following equation:

$$\sigma_N = f_r^0 \left[\left(\frac{rD_b}{D + rsD_b}\right)^{rn_d/m} + \frac{rD_b}{D + rsD_b}\right]^{1/r} \tag{6}$$

where n_d = number of spatial dimensions in which the structure is scaled ($n_d = 1$, 2 or 3), m = material constant = Weibull modulus.

Note that for $m \to \infty$ (and $s = 0$) Eq. (6) coincides with the foregoing energetic (deterministic) Eq. (4). For $D \gg D_b$ or $D_b = 0$ (and $s = 0$) Eq. (6) becomes

$$\sigma_N = f_r^0 (D_b/D)^{n_d/m} \tag{7}$$

and thus one recovers the classical formula for Weibull size effect as the limit case.

3.3 *Experimental Studies*

The energetic-statistical theory of flexural strength of laminates was checked and calibrated from the existing test data in the literature. Results are shown in Fig. 5 presenting the optimum fit of the existing test data on flexural strength versus relative size, in which ω is an unbiased estimate of the coefficient of variation corresponding to the standard error of regression and r appears in Eq. (3).

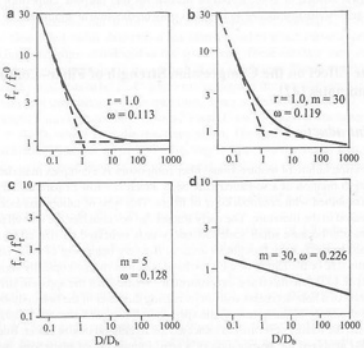

Fig. 5 Optimum fits of existing test data on modulus of rupture versus relative size, in dimensionless coordinates, by (**a**) deterministic energetic formula; (**b**) energetic-statistical formula; (**c**) Weibull size effect formula with $m = 5$; and (**d**) Weibull size effect formula with $m = 30$

3.4 Conclusions

From the results, the following conclusions may be drawn:

1. The size effect on the flexural strength of laminates appears to be primarily energetic (deterministic) rather than statistical, except possibly for very large thicknesses for which the statistical size effect might also be significant. This further implies that fracture mechanics, rather than some strength criterion (or material failure criterion expressed in terms of stresses and strains), needs to be used for evaluating the strength of laminates. The fracture mechanics approach must take into account the quasibrittle (or cohesive) nature of fracture.
2. The statistical theory is inapplicable for the prediction of the size effect of the flexural strength of composite laminates.
3. The existing experimental data support the applicability of both the energetic theory and the energetic-statistical theory. However, the available data do not suffice to demonstrate that the energetic-statistical theory is better than the energetic theory (which is a special case). Experimental data of a broader size range or lower scatter, or both, would be needed for that purpose. Superiority of the energetic-statistical theory so far relies only on theoretical arguments.

4 Size Effect on the Compression Strength of Fiber–Composite Laminates [42]

4.1 Introduction

Compression failure of unidirectional fiber composites is a complex material failure involving formation of a so-called kink band which is a row of parallel axial shear cracks combined with microbuckling of fibers. This type of failure has extensively been studied in the literature. The early studies did not consider the size effect. This seems natural because small-scale laboratory tests indicated no size effect and the maximum load has been thought to occur at the very beginning of microbuckling, before the size or the length of the kink band becomes macroscopically significant. Soutis et al. [43] calculated and experimentally verified that the apparent strength in the vicinity of a hole decreases with an increasing diameter of the hole. Although geometric similarity of the hole with the specimen dimensions was not maintained in these tests, the results nevertheless indicated the likelihood of size effect. Budiansky et al. [44] analyzed the propagation of a semi-infinite out-of-plane kink band, approximating the band with a crack whose face is allowed to overlap in compression. Their analysis clearly suggests the existence of a size effect on the nominal strength of geometrically similar specimens.

In the present study the effect of structure size on the nominal strength of unidirectional fiber–polymer composites, failing by propagation of a kink band with fiber microbuckling, is analyzed experimentally and theoretically. Tests of novel geometrically similar carbon-PEEK specimens are conducted. They confirm the possibility of stable growth of long kink bands before the peak load, and reveal the existence of a strong deterministic size effect.

4.2 Experimental

Failure by kink band propagation is usually combined with axial splitting-shear cracks and delaminations. For the present investigation the shape of the specimen and the type of material should be properly selected to lead to pure kink band failure even for very large sizes. A carbon fiber PEEK (poly-ether-ether-keton)/thermoplastic matrix polymer composite was chosen. This material is less brittle than carbon/epoxy composites and leads to more stable failures. Thus, if a size effect is found to exist in this type of composite, it should also exist in a more pronounced form in more brittle composites, such as the carbon fiber–epoxy composites. To exclude the effect of random variation of material strength over the specimen volume, notches were introduced in the specimens to ensure that failure begins in a desired place and not at diverse locations where the material is statistically weakest. One-sided, rather than two-sided, starter notches which cause a stable path of the kink band were introduced in the specimens. These notches were made inclined and not perpendicular to the surface of the specimens. The inclination angle was found by trial tests to be 25.4°, equal to the angle of the out-of-plane kink band.

The in-plane dimensions of the specimens were scaled at the ratio 1:2:4, while the thickness b was kept constant ($b = 12.7\,\text{mm}(0.5\,in.)$) (Fig. 6). The notch length was $a_0 = 0.3D$, where D is the specimen width. The notch was machined with a diamond bladed band saw up to 95% of its length. Then the notch was sharpened at the tip by a cut whose depth is 5% of the notch depth. The cut was machined with a 0.2 mm diameter diamond-studded wire, and thus the crack tip radius was 0.1 mm in all the specimens. The depth a_0 of the notch considered for scaling and in the analysis included the depth of the wire saw cut.

The specimens were prepared by compression molding of 100 plies of sheets 304.8 × 304.8 mm, 0.05 mm thick of carbon/polymer prepreg sheets supplied by Fiberite, Inc. under temperature 391°C (735°F) and pressure 0.69 MPa, using the manufacturer recommended curing cycle. After the specimens were cut from the sheets at the proper dimensions they were provided with massive end caps made of 1,040 hot rod steel, to which they were glued by epoxy. To ensure proper alignment, the end caps were glued only after the specimen had been installed under the loading platens of the testing machine. The end plates were restrained to prevent any rotations. The specimens were tested under a controlled stroke rate of 1.27×10^{-4} mm/s. Following initiation at the notch tip, the kink band propagated stably on both the front and back sides of the specimen. At the beginning of propagation the kink band on one side was usually slightly longer than that on the other side. However, during propagation the shorter band on one side would soon catch up with the longer band on the opposite side.

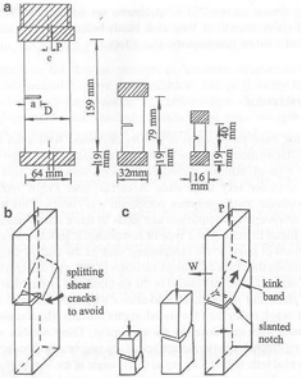

Fig. 6 (a) Geometrically similar single-edge notched carbon-PEEK (poly-ether-ether-keton) specimens tested, and scheme of loading; (b) specimen with an orthogonal notch exhibiting undesirable failure (splitting shear cracks); and (c) transversely slanted notches achieving pure kink band failure

The nominal strength of the specimen is defined as

$$\sigma_N = P/bD \tag{8}$$

where

P = maximum load measured
b = specimen thickness
D = specimen width (chosen as the characteristic dimension).

The specimen width D is chosen as the characteristic dimension. Fig. 7 shows the test results plotted in the form of $\log \sigma_N$ versus $\log D$. The stress–strain diagrams of the small, medium and large specimens are given in Fig. 8, where the average stress is defined over the ligament as $\sigma_L = \sigma_N D/(D - a_0)$ and the average axial strain ε is determined as the stroke of the piston divided by the length between the platens. Note that the load-deflection diagrams exhibit a post-peak stress drop rather than a horizontal yield plateau at peak load. This fact alone suffices to demonstrate that a fracture-type approach (or a nonlocal damage approach) is required.

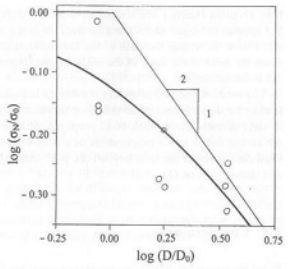

Fig. 7 Results of tests of nominal strength of carbon-PEEK specimens (data points) and their optimum fit by the size effect law of Bazant

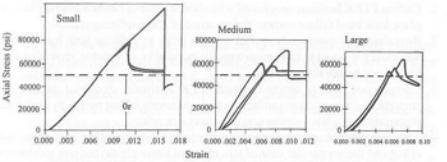

Fig. 8 Load-deflection diagrams of carbon-PEEK specimens tested

Furthermore, these diagrams reveal the existence of a terminal yield plateau, which confirms the existence of a finite residual stress across the kink band. The experimental results of Fig. 7 indicate a downward trend of nominal strength versus characteristic dimension of the specimens. The downward slope is quite steep and closer to the slope $-1/2$ corresponding to LEFM than to the horizontal line corresponding to the strength theory. This indicates a strong size effect, even though the PEEK matrix is relatively ductile.

Note in Fig. 7 that one of the small specimens, corresponding to the upper left data point, did not develop a kink band but failed by a vertical shear crack that started from the notch tip and produced axial splitting. This point was not excluded, but retained in the data because it is the highest point in the data set, and the load that would cause the kink band failure of this specimen must have been at least as high as this point. The test results exhibit considerable random scatter. This is, however, typical of compression failure of fiber composites (because of their strong sensitivity to fiber misalignment). For this reason, the size effect would not have

been revealed clearly if the size range were less than 1:4. The present size range of 1:4 appears to be just about the minimum for being able to clearly demonstrate the size effect. To reduce the ratio of the inevitable scatter band width to the range of sizes, the ratio of the sizes of the smallest and largest specimens should be at least 1:8 in future testing.

The rotation restraint boundary conditions imposed at the ends of the specimens lead to the development of an unknown moment causing the compression resultant to shift laterally during kink band propagation. However, the end restraint has the advantage that a stable propagation of a long kink band is possible and the post-peak deformations are well beyond the peak load while the residual stress plateau and stresses can be observed.

4.3 Conclusions

From the results, the following conclusions may be drawn:

1. Carbon-PEEK laminate specimens with slanted notches can achieve pure out-of-plane kink band failure without the presence of shear splitting cracks.
2. Restraining specimen ends against rotation helps to stabilize kink band growth and makes it possible to demonstrate the possibility of a stable growth of long kink bands before the peak load.
3. Compression tests of notched carbon-PEEK laminates show that the nominal strength of geometrically similar notched specimens failing purely by kink band propagation exhibits a strong non-statistical size effect.
4. The size effect observed is transitional between the asymptotic case of no size effect and the asymptotic case of size effect of linear elastic fracture mechanics, which is governed by energy release.
5. The results of the present carbon-PEEK tests roughly agree with the approximate general size effect law proposed by Bažant.
6. The results of the present study suggest that the current design practice, in which the compression failure is predicted on the basis of strength criteria which miss the size effect, is acceptable only for small specimens or structural parts. However, for large structural parts the size effect should be taken into consideration.

5 Size-Effect on Fracture of Polymeric Foams [45]

5.1 Introduction

Cellular foams are frequently used as core materials in sandwich construction. They are relatively inexpensive and consist of a vast variety of foamed plastics and metals with varying densities, elastic properties and strengths. Commercially

available plastic foams are made of polyvinyl chloride (PVC), polyurethane (PUR), and polystyrene, among others. Metallic foams are usually made of aluminum. The properties of foams depend on the structure of the cell, the density and the material of which they are made. A detailed characterization of their mechanical behavior is essential for their efficient use in structural applications. A thorough analysis of the mechanical properties of plastic foams is given in the book by Gibson and Ashby [46]. They presented simple micromechanical equations based on mechanics of materials analysis to relate the properties of the foam to the structure of the cells and the properties of the cell material. Gdoutos et al. [47] studied the mechanical behavior of cellular foams under multiaxial stresses. Furthermore, Gdoutos and Abot [48] analyzed the indentation behavior of foams.

The objective of this work is to study the effect of structure size on the nominal strength of closed-cell PVC foam (Divinycell H100). Two types of size effect are considered: Type I, characterizing the failure of structures with large cracks or notches, and Type II, characterizing the failure at crack initiation.

5.2 Experimental

The material of the specimens was a PVC closed-cell rigid foam under the commercial name Divinycell H100 with density 100 kg/m^3. The specimens were cut from the same plate and had a thickness $b = 25{:}40$ mm (1 in.). To determine the size effect in tensile (model I) fracture, geometrically similar specimens in two dimensions with length-to-width ratio 5:2 were selected. The width of the specimens was $D = 6.35$, 43.94 and 304.80 mm (Fig. 9). In order to ensure that failure begins at a desired place and not start at diverse locations where the material is statistically the weakest (which could cause a Weibull-type size effect), notches were introduced in the specimens. The width of the notches was 1.00 mm and depth 0.4 D. The tip of the notch was sharpened by a blade having the thickness of 0.25 mm. Compressive tests were also performed using the same specimens but only of the middle size. To avoid the opposite faces of the notch from getting in contact before the maximum compressive load is reached, the notch was widened with a band saw to a wedge shape of width 25 mm at the notch mouth. The notch tip was sharpened by a razor blade. The ends of specimens were glued by epoxy to very stiff steel platens which were gripped in the loading machine, with any rotation of the ends prevented.

The specimens were loaded in tension in a servo-hydraulic machine. To minimize the viscoelastic effects due to differences in the loading rate, the displacement rate of the platens was uniform throughout the test and was chosen such that the specimens of any size would reach the maximum load within about 5 min. The displacements were measured by LVDT gages mounted across the notch mouth spanning, in the case of tension tests, a base length of 11.50 mm. A typical load – displacement curve is shown in Fig. 10.

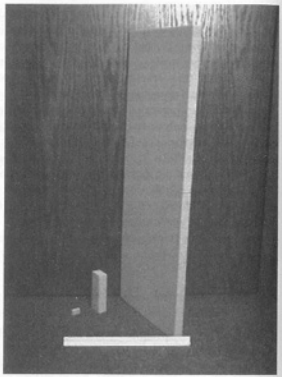

Fig. 9 Foam specimens geometrically similar in two dimensions for tensile fracture test (Divinycell H100)

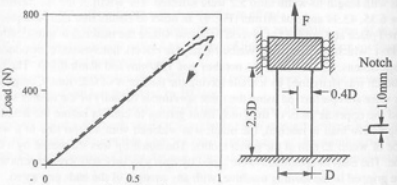

Fig. 10 A typical load-δ_{CMOD} curve in the tensile fracture test

5.3 *Size Effect*

Cellular foams have micro-structural inhomogeneities, such as cells and finite fracture process zones, and therefore, must exhibit a size effect, unless the structural dimensions are far larger than the characteristic length of the foam. Fig. 11 presents

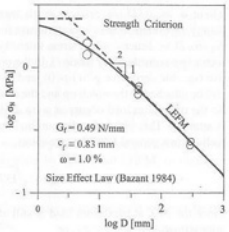

Fig. 11 Results of size effect tests of nominal strength of geometrically similar prismatic Divinycell H100 foam specimens with similar one-sided notches subjected to tension

a plot of the nominal strength $\sigma_N = P_{max}/bD$ versus log D, where P_{max} is the failure load, and D and b the specimen width and thickness. Note in Fig. 11 that there is a very strong size effect. This size effect cannot be explained by the Weibull statistical theory. In that case the plot of log σ_N versus log D, corresponding to the typical values of Weibull modulus, would have to be a straight line of a slope equal to $-2/m$ where m is the Weibull modulus characterizing the coefficient of variation of local material strength. Since its value is typically between 15 and 30, this straight line would have to have a slope between -0.03 and -0.07. However, the size effect observed in Fig. 11 is much stronger than that, overpowering any possible statistical size effect, and is of deterministic character.

According to Bažant [49] there are three types of deterministic (energetic) size effect. Type I is caused by relatively large notches or fatigued (stress-free) cracks formed prior to maximum load; type II occurs at crack initiation and is caused by a relatively large fracture process zone (FPZ); and type III is caused by large stable crack growth in structures of initially negative geometry; it is quite similar to Type II and will not be considered here. Note in Fig. 11 that the experimental results are very close to the straight line of downward slope $-1/2$, which indicates that the material behaves in an almost brittle manner. The term "brittle" is understood as the adherence to LEFM, while the term "quasibrittle" refers to nonlinear cohesive softening (non-ductile) fracture with a large FPZ, deviating from LEFM.

According to the size effect method of measuring nonlinear fracture properties [50–52], the location in Fig. 11 of the asymptote of slope $-1/2$ determines the fracture energy G_f of the material, and the rate at which this asymptote is approached determines the effective size of the FPZ, c_f, representing the distance from the actual crack tip to the tip of an equivalent LEFM crack, which lies roughly in the middle of the FPZ and can be precisely defined as the tip location that gives the best LEFM fit of the actual size effect curve. The energy release rate in LEFM may always be expressed as

$$G = K_I^2/E = \sigma_N^2 g(\alpha) D/E \tag{9}$$

where $\alpha = a/D$ = relative crack length, a = actual crack length, $g(\alpha) = [k(\alpha)]^2$ = dimensionless energy release function of relative crack length α, $k(\alpha) = K_I/\sigma_N D$ = dimensionless stress intensity factor, and K_I = actual stress intensity factor (we consider only mode I). In the present case, the fracture geometry is positive (i.e., the derivative $g'(\alpha) > 0$), and in that case the FPZ at maximum load must still be attached to the notch tip and the crack begins to propagate at decreasing load. So the maximum load occurs as soon as the crack propagation condition $G = G_f$ is attained. This yields for the nominal strength $\sigma_{Nu} = \sigma_N$ at maximum load the well-known general LEFM expression:

$$\sigma_{N_u} = \sqrt{EG_f/g\,(\alpha)\,D} \tag{10}$$

Since the FPZ at maximum load is still attached to the notch tip, we may use the approximation $a = a_0 + c_f$, or

$$\alpha = \alpha_0 + \theta \text{ with } \alpha_0 = a_0/D, \theta = c_f/D \tag{11}$$

where a_0 is the length of notch or preexisting traction-free crack; c_f = material constant ≈ half-length of the FPZ.

The size effect for geometrically similar specimens (i.e., specimens for which α_0 = constant) could be simply described by substituting $\alpha = \alpha_0 + \theta$ into Eq. (10). However, such an approximation would be valid only for large sizes D because for small enough D the argument of $g(\alpha)$ becomes larger than the range of α for which $g(\alpha)$ is defined. To find a size effect law applicable for all sizes, we write an asymptotic expansion in terms of $1/D$:

$$g\,(\alpha) = g\,(\alpha_0 + c_f/D) = g\,(\alpha_0) + g'\,(\alpha_0)\,c_f/D + (\cdot\cdot)/D^2 + \tag{12}$$

Truncating it after the second term, we get from Eq. (10) the size effect law proposed by Bažant [10] and Bažant and Kazemi [47]:

$$\sigma_{N_u} = \sqrt{\frac{E'G_f}{\left[g\,(\alpha_0) + g'\,(\alpha_0)\,c_f/D\right]D}} = \frac{\sigma_{N_0}}{\sqrt{1 + D/D_0}} \tag{13}$$

in which,

$$\sigma_{N_0} = \sqrt{\frac{EG_f}{g'\,(\alpha_0)\,c_f}}, \quad D_0 = c_f\frac{g'\,(\alpha_0)}{g\,(\alpha_0)} \tag{14}$$

D_0 represents the transitional size delineating the brittle behavior from nonbrittle (ductile) behavior and corresponds to the intersection of the asymptotes in Fig. 11: D_0 and σ_{N0} are constant because, owing to geometric similarity, α_0 is a constant for all the specimens tested. The ratio $\beta = D/D_0$ is called the brittleness number [50]; $\beta \gg 1$ means a very brittle response, close to LEFM, and $\beta \ll 1$ means a very ductile response. To be able to identify the material fracture parameters from

size effect tests, the range of β must be sufficiently broad (in this regard, note that variation of the ratio $g'(\alpha)/g(\alpha)$ due to changes in geometry, e.g., the relative notch depth, helps to increase the range of β.

Based on the above analysis and using the data of Fig. 11, the following values were obtained for the foam under study:

$$G_f = 0{:}49\,\text{N/mm},\ c_f = 0{:}83\,\text{mm},\ K_c = 6{:}53\,\text{N/mm}^{3/2},\ \delta_{CTOD} = 0{:}10\,\text{mm}$$

Knowledge of these material parameters makes it possible to analyze the size effect due to fracture in the core of a sandwich plate by equivalent LEFM, or cohesive crack model, or crack band model.

From compression tests of V-notched specimens it was found that there is no size effect, and therefore, the usual plasticity analysis can be used to describe the compressive failure of PVC cellular foams.

Data of Zenkert and Bäcklund [53] on tests of beams made of Divinycell H200 under three-point bending were fitted with the sized effect law of Bažant. Results are shown in Fig. 12. The specimens have thickness $b = 30$ mm, span/depth ratio,

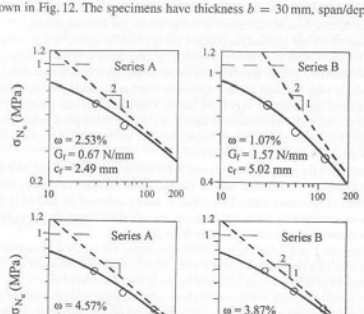

Fig. 12 Fit of Zenkert and Bäcklund's [53] results for three-point bend beams by Bazant's size effect law (solid line). Dashed line: LEFM. Dash-dot line: strength criterion. Series A (left) and B (right) pertain to different temperature conditions and material from different blocks. *Top*: Fits when G_f and c_f are optimized separately for each series. *Bottom*: Fits when c_f is forced to be the same for both series while G_f values are allowed to be different

$L/D = 4$, and ratio of notch length to specimen depth, $a = 0.5$, but different beam depths $D = 30$, 60 and 120 mm. Two series of size effect tests, labeled A and B, were performed by using specimens cut from two different blocks of the foam and subjected to slightly different temperature conditions. There were appreciable differences between these two series, which must be due to differences in temperature conditions as well as notoriously high randomness of foam properties and perhaps uncontrollable differences in specimen manufacture. The randomness is documented by very high scatter of the fracture toughness values, K_{Ic}, measured by Zenkert and Backlund on specimens cut from different blocks of material.

5.4 Conclusions

1. Notched closed-cell PVC foam (Divinycell H100) panels exhibit a strong size effect. It agrees well with the size effect law proposed by Bažant [10], which describes a smooth transition between the asymptotic case of no size effect and the asymptotic case of size effect of linear elastic fracture mechanics.
2. The size effect law permits the fracture energy and the effective fracture process zone length of foam to be easily identified by measuring only the maximum loads of geometrically similar notched specimens of sufficiently different sizes.
3. The single edge-notched tension specimen fixed at the ends provides a suitable fracture test specimen for very light foams. This specimen fails purely by tensile fracture, while other specimens of light foam, such a three-point bend beams, are plagued by simultaneous compression collapse of foam cells at places of load application, which distorts the results.
4. Evaluation of the energy release function for this test specimen must take into account the effect of the lateral shift of the axial load resultant caused by rotational restraints at specimen ends. This effect is easily captured by LEFM if the end rotations canceled by rotational restraint are calculated from the stress intensity factor expression as a function of crack length.
5. Conclusions 1 and 2 for the size effect also apply for notched three-point bend specimens of a heavier foam (Divinycell H200). Realistic values of the fracture parameters of this foam are obtained by using the size effect law.
6. Foam specimens with V-shaped notches (with an angle wide enough to prevent the notch faces from coming into contact) exhibit no size effect in compression. This implies that the cell collapse at the tip of the notch must be essentially a yielding process rather than a softening damage process.
7. The results demonstrate that the current design practice, in which the tensile failure of foam is generally predicted on the basis of strength criteria or plasticity, is acceptable only for small structural parts. For large structural parts the size effect must be taken into account, especially if the foam has large fatigued cracks or large damage zones prior to critical loading to failure.

6 Size Effect on Compressive Strength of Sandwich Panels [54]

6.1 Introduction

A sandwich structure consists of two external thin, strong, stiff facings bonded to a thick light-weight and weaker core. The core carries the through-the-thickness shear loads, while the facings resist in-plane and bending loads. The high specific strength and specific stiffness of sandwich construction coupled with outstanding thermal and acoustic insulation make it ideal in structural design. Sandwich beams may fail in several ways including tension or compression failure of the facings, shear failure of the core, wrinkling failure of the compression facing, local indentation, debonding of the core/facing interface and global buckling. Following initiation of failure by a specific failure mode, interaction of failure modes may occur and failure could progress by another failure mode.

Sandwich materials are quasibrittle and exhibit size effect. While in small structural parts the size effect is negligible, large structures display pronounced size effect that should be taken seriously into account in structural design. Quasibrittle behavior automatically implies a significant deterministic size effect of the energetic type, whose cause is the energy release associated with stress redistribution prior to maximum load, engendered either by a large FPZ (type 1 size effect) or by a large crack (type 2 size effect).

It is the objective of this work to study the size effect in sandwich panels subjected to eccentric axial compression. The sandwich panels consist of a closed-cell polyvinyl chloride foam, and woven glass-epoxy laminate facesheets. The panels had small notches which caused the failure to occur in only one place in the specimen, and failed by kink band propagation.

6.2 Experimental

The specimens had the form of prismatic sandwich panels of rectangular cross section (Figs. 13 and 14). The core material was a PVC cellular foam under the commercial name Divinycell H250, of density 250 kg/m^3. The facesheets were glass-epoxy laminates (7,781 style satin weave glass and Bryte 250 epoxy resin), consisting of several plies. The prepreg material was manufactured by hot-melt film coating and was oven cured under vacuum consolidation. Two types of skins were used in the tests: porous and nonporous The porosity was 3% to 5%, which is representative of manufacturing defects. The specimens were designed so that failure by skin wrinkling and global buckling could not take place. The modulus of elasticity of the core was $E_c = 400$ MPa and the axial modulus of the orthotropic skins (nonporous) was $E_s = 24{,}300$ MPa. The compression strength values were about 390 MPa (nonporous skin) and 320 MPa (porous skin), and 5.7 MPa for the foam core.

Fig. 13 Test specimen

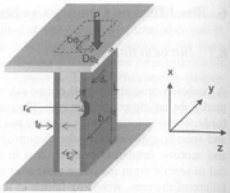

Fig. 14 Specimens showing size variation

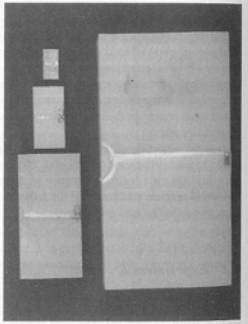

The specimens were geometrically scaled in three dimensions to four different sizes of ratio 1:2:4:8. They were subjected to a doubly eccentric axial load in order to ensure that only one FPZ develops within the cross section. Centric loading might be more difficult to interpret because several interacting FPZs could be developing simultaneously in the cross section prior to the maximum load. The ratios e_x and e_y of load eccentricities to D and b (the specimen thickness and width) are kept constant. To scale the laminate skins, the number of plies n of the facesheets is increased progressively, and is $n = 2, 4, 8$, and 16 for the respective four specimen sizes. The load is applied through rigid end plates clamped to the ends of the specimen. To ensure that the specimens fail by deterministic, and not statistical, size

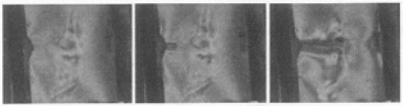

Fig. 15 Development of fracturing compressive kink band at the notch in the laminate skin

effect, semi-circular notches of radius r_n and notch depth d_n scaled in proportion to D were introduced at the most highly stressed edge of the facesheets. Thus, failure of the specimens would initiate at the radius of the notches.

Failure of sandwich panels consists of horizontal propagation of a softening fracturing kink band. In order to detect this failure mode a photoelastic coating was bonded to the specimen. Fig. 15 presents the photoelastic fringe pattern during loading. Kink band propagation with microbuckling causes a reduction of the normal stress transmitted across the band, which is properly regarded as a phenomenon of cohesive fracture, characterized by a certain kink band fracture energy, implying a certain characteristic length of the kink band FPZ, and a finite residual stress on the softening stress-displacement relation of the kink band. The results show that this mode of failure generally produces a significant energetic size effect, and so it is no surprise that a pronounced size effect is exhibited by the present tests.

6.3 *Size Effect*

According to the deterministic size effect theory developed by Bažant [49] the allowable strength limit, σ_N, is given by:

$$\sigma_N = \sigma_\infty (1 + r D_b/D)^{1/r} \quad (Type\ 1) \tag{15}$$

$$\sigma_N = \sigma_0 (1 + D/D_0)^{-1/2} + \sigma_r \quad (Type\ 2) \tag{16}$$

where σ_∞, r, D_b, D_0, σ_0, and σ_r are constants (related to the geometry and properties of the material). The type 1 size effect law applies to failures at fracture initiation from a smooth surface, and type 2 to failures when a large notch or a large crack is present at maximum load. Parameter σ_r represents the residual nominal strength of the specimen, due to frictional-plastic resistance after the fracture is fully formed. Usually $\sigma_r = 0$ for tensile failures, but for compression failure σ_r can be nonzero.

The allowable strength limit σ_N represents the maximum stress calculated from the elastic theory of bending, and is defined as:

$$\sigma_N = cP/bD \tag{17}$$

where P is the maximum load, $D = t_c + 2t_f$, where t_c and t_f represent the thickness of the core and facesheet, b is the width of the sandwich panel and c is given by:

$$c = \frac{1}{2t_f/D + E_c t_c/E_f D} + \frac{6e_y}{2t_f/D + E_c t_c/E_f D} + \frac{6e_z}{(1 - t_c^3/D^3) + E_c t_c^3/E_f D^3} \tag{18}$$

For the present sandwich geometry, the numerical value of c was 10.92. Because the present specimens have a sizeable notch, the type 2 size effect dominates and Eq. (16) applies.

The sandwich specimens were compressed at a constant displacement rate, for each size equal to 0.01 in./min. The viscoelastic effects on σ_N were expected to be unimportant. For each test the maximum load was measured. The values of measured nominal strength σ_N, calculated from the maximum load P with $c = 10.92$, are shown by the data points in Fig. 16. In the same figure the optimum fits by the type 2 size effect law of Eq. (16) are shown by continuous lines and the asymptotes of this law are also marked. In the plots on top, it is assumed that there is no residual strength ($\sigma_r = 0$), while in the plots at the bottom, the residual strength σ_r is finite. While Fig. 16 shows the data in logarithmic scales, Fig. 17 shows the same data in the plots of $1/\sigma_N^2$ or $1/(\sigma_N - \sigma_r)^2$ versus D/D_0, which are useful because Eq. (16) gets transformed, in such coordinates, to a linear regression plot. In such a plot, the

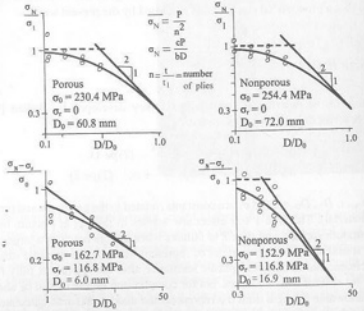

Fig. 16 Measured values (data points) of nominal strength σ_N of eccentrically compressed sandwich prisms of various sizes (thicknesses) D, plotted as $\log(\sigma_N - \sigma_r)$ versus $\log D$, and their fit by type 2 size effect law, Eq. (16). *Left*: Porous laminate skins from standard manufacture. *Right*: Nonporous laminate skins

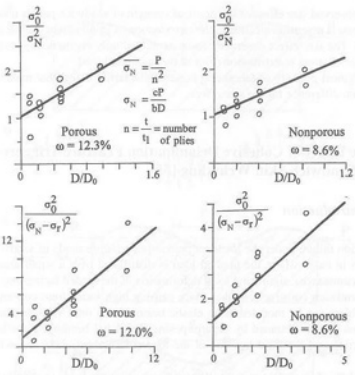

Fig. 17 The same data and fits as in Fig. 16, but replotted as $\sigma_0^2(\sigma_N - \sigma_r)^{-2}$ versus D/D_0 to obtain a linear regression plot

optimum (least-squares) fit of the data by Eq. (16) is easily obtained, along with the coefficient of variation ω of the data deviations from the regression line. The optimum values of D_0, σ_0, and σ_r obtained by regression are listed in each figure.

The data plots in Figs. 16 and 17 make it clear that the size effect exists and is quite pronounced. Therefore, the current design procedures, which are based on the concept of material strength, are not justified for larger sandwich structures under compression.

6.4 Conclusions

From the results, the following conclusions may be drawn:

1. The experimental results indicate that compressive failure of laminate-foam sandwich plates exhibits a significant size effect.
2. The thickness range of the tests performed corresponds to the thicknesses of load-bearing fuselage panels of small aircraft, while application to large ship structures will require extrapolation of the measured size effect.

3. The observed size effect of the nominal strength of sandwich panels under compression is deterministic, due to the introduction of small notches in the laminate skins. The size effect observed can be explained only energetically, as a consequence of stress redistribution prior to the maximum load.
4. The typical porosity of facesheets is a manufacturing defect that makes no significant difference for the size effect.

7 Size Effect of Cohesive Delamination Fracture Triggered by Sandwich Skin Wrinkling [55]

7.1 Introduction

Indentation failure under the load is a predominant failure mode of sandwich construction in cases where the applied load is distributed over a small area. Under such circumstances, significant local deformation of the loaded facing into the core of the sandwich construction takes place causing high local stress concentrations. The problem can be modeled as an elastic beam resting on a Winkler foundation. The stress field is obtained by superimposing the global bending of the sandwich construction and the local bending of the loaded face sheet about its own neutral axis.

Buckling of imperfect quasibrittle structures generally leads to snapthrough instability which typically exhibits size effect on the nominal strength. The objective of this section is to show that skin imperfections (considered proportional to the first eigenmode of wrinkling) lead to strong size dependence of the nominal strength. For large imperfections, the strength reduction due to size effect can reach 50%. Dents from impact, though not the same as imperfections, might be expected to cause as a similar size effect. A secondary objective is to assess the size effect on the postpeak energy absorption, important for judging survival under blast or dynamic impact.

7.2 Size Effect

The analysis of delamination in sandwich structures subjected to pure bending (Fig. 18a) can be simplified by modeling the skin as an axially compressed beam supported by a softening foundation consisting of independent continuously distributed nonlinear springs. This problem for bilinear elastic-softening response of the foundation was solved by Bažant and Grassl [55]. For the case when the wavelength of skin wrinkling $L_{cr} \ll h$, where h represents the core thickness, the core may be regarded as an infinite half-space. The reason is that the alternating tractions applied on the core by the periodically wrinkled skin (Fig. 18b) are self-equilibrated over a segment of length $2L_{cr}$ where L_{cr} is the half wavelength of skin buckling

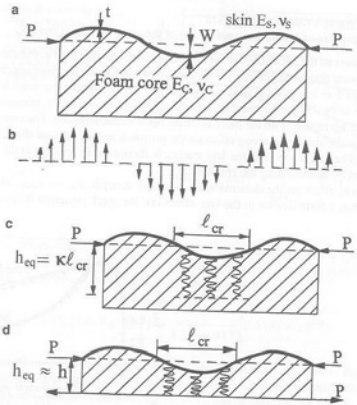

Fig. 18 (a) The deflection of the top skin; (b) equilibrated stress acting on the foam; (c) equivalent height for shortwave; and (d) long wave wrinkling

(Fig. 18c). Therefore, according to the St. Venant principle, the stresses caused by periodic wrinkling must exponentially decay to nearly zero over a distance from the skin roughly equal to $2L_{cr}$. On the other hand, when the critical wavelength $L_{cr} \gg h$ (Fig. 18d) the sandwich beam is subjected to bending moment only (i.e., with no axial force). Then the opposite skin is under tension and may be approximated as a rigid base, with no deflection. The transverse compressive stress in the core is now almost uniform, and the foundation stiffness is constant (independent of the critical wavelength).

Consider the load parameter λ defined by

$$x = X\left(\frac{E_s I_s}{K}\right)^{-1/4}, \quad \lambda = \frac{1}{2}P(KE_s I_s)^{-1/2} \tag{19}$$

where:

P = axial load in the beam (per unit width)
K = spring stiffness of the foundation per unit length

E_s = Young's modulus of the skin
I_s = moment of inertia (per unit width) of the cross section of the skin

The effect of the structure size on the relation between the load parameter λ and the mid-point displacement $w_a = w\,(l/2)$ is shown in Fig. 19 for three imperfection amplitudes $\delta = 0.1, 1, 2$ (in which, $l = L(E_s I_s/K)^{-1/4}$, where the beam length L is chosen to be $17L_{cr}$. As one can see, the analytical results are in reasonable approximate agreement with the more accurate finite element results. The comparison shows that the size has a strong effect on the postpeak part of the load-displacement relation. The larger the size, the less energy is dissipated in relation to the energy dissipated by delaminating the entire skin.

The size effect on the dimensionless nominal strength, $\lambda_N = \lambda_{max}$, shown in Fig. 20, has a form similar to the size effect law for crack initiation in quasibrittle

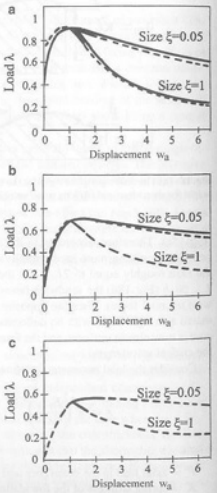

Fig. 19 Load λ versus the midpoint displacement w_a obtained with the softening foundation model and the finite element model for the imperfections: (**a**) $\lambda = 0.1$; (**b**) $\lambda = 0.5$; and (**c**) $\lambda = 1$ for two sizes ($\lambda = 1$ and $\lambda = 0.05$)

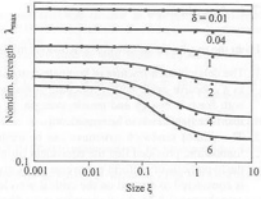

Fig. 20 Comparison of the size effect law in Eq. (20) with the nominal strength – size curves obtained from the softening foundation model for different imperfections

structures, which reads $\lambda_N = \lambda_\infty[1 + 1/(k + \xi)]$, where λ_∞ has the meaning of nominal strength of an infinitely large structure. This law, however, is not directly applicable in this case. Therefore, a generalized law of the form

$$\lambda_N(\delta, \xi) = \lambda_\infty(\delta)\left[1 + \frac{1}{k(\delta) + \alpha\xi^b}\right],\ k(\delta) = c\delta^{-4} \tag{20}$$

is proposed here, with constants a, b, c, d and parameters λ_∞ and k, depending on the imperfection amplitude δ. For large sizes ($\xi \to \infty$), the nominal strength is decided by initiation of cohesive crack ($w = 1$), and in that case we obtain

$$\lambda_N(\delta, \infty) = \lambda_\infty = 1/(1 + \delta) \tag{21}$$

Note that here the large-size limit does not correspond to LEFM, which is the case for type 2 size effect [56], seen in specimens with notches or large stress-free cracks. Rather, in the absence of preexisting delamination crack, we see a particular case of type 1 size effect [56] because the geometry is positive causing failure to occur at crack initiation.

For small sizes the nominal strength turns into:

$$\lambda_N(\delta, 0) = \lambda_\infty(\delta)\left[1 + \frac{1}{k(\delta)}\right] \tag{22}$$

Parameters a, b, c, d in Eq. (20) are determined as the optimal fits of numerical results using the Marquardt–Levenberg algorithm for nonlinear least-squares optimization. The size effect law in Eq. (20) using these parameters is compared to the results of the softening foundation model in Fig. 20. The approximation is seen to be satisfactory.

7.3 Conclusions

From the results, the following conclusions may be drawn:

1. The delamination fracture of laminate-foam sandwich structures must be treated as a cohesive crack with a softening stress-separation relation characterized by both fracture energy and tensile strength. In contrast to LEFM, no preexisting interface flaw needs to be considered.
2. The skin of sandwich structures can be treated as a beam on elastic-softening foundation, provided that the equivalent (or effective) core depth h_{eq} for which the hypothesis of uniform transverse stress gives the correct foundation stiffness is considered to depend on the critical wavelength L_{cr} of skin wrinkles; $h_{eq} = core$ thickness h for the asymptotic case of long wave wrinkling ($L_{cr}/h \to \infty$), while (because of St. Venant principle) h_{eq} is proportional to L_{cr} for the asymptotic case of shortwave wrinkling ($L_{cr}/h \to 0$).
3. Although the nominal strength of sandwich structures failing by wrinkling-induced delamination fracture is size independent when there is no imperfection, it becomes strongly size dependent with increasing imperfection. A size effect causing strength reduction by 50% is possible for larger imperfections. Dents from impact may be expected to have a similar effect, even though they are not merely geometrical imperfections (because of being usually accompanied by initial delamination).
4. There is also a strong size effect on post peak energy absorption by a sandwich structure, both in the presence and absence of imperfections. This is important for impact and blast resistance.

Acknowledgment Most of the work reviewed in this paper was sponsored by ONR from the program directed by Dr. Y.D.S. Rajapakse during the years 1994–2005.

References

1. Timoshenko SP (1953) History of the strength of materials, McGraw Hill, New York
2. Irwin GR, Wells AA (1965) A continuum mechanics view of crack propagation. Metal Rev 10: 223–270
3. Galileo Galilei L (1638) Discorsi e Dimostrazioni Matematiche intorno à due Nuove Scienze, Elseviriı, Leiden; English transl. by Weston T, London (1730), pp. 178–181
4. Mariotte E (1686) Traité du mouvement des eaux, posthumously edited by M de la Hire; transl. by Desvaguliers JT, London (1718), p. 249; also Mariotte's collected works, 2nd edn., The Hauge, 1740
5. Griffith AA (1921) The phenomena of rupture and flow in solids. Phil Trans Royal Soc Lond A221: 163–198
6. Griffith AA (1924) The theory of rapture. In: Proceedings of the First International Congress of Applied Mechanics, Delft, pp. 55–63
7. Stanton TE, Batson RGC (1921) Proc Inst Civ Eng 211: 67–100
8. Weibull W (1939) Phenomenon of rupture in solids. Proc Roy Swedish Inst Eng Res (Ingeniorsvetenskaps Akad Handl) 153: 1–55

9. Bažant ZP (1983) Fracture in concrete and reinforced concrete. In: Bažant ZP (ed.), Preprints Prager Symposium on Mechanics of Geomaterials: Rock, Concrete, Soils, Northwestern University Press, Evanston, IL, pp. 281–319
10. Bažant ZP (1984) Size effect in blunt fracture: concrete, rock, metal. J Eng Mech ASCE 110: 518–535
11. Bažant ZP (1982) Crack band model for fracture of geomaterials. In: Eisenstein, Z (ed.), Proceedings of the 4th International Conference on Numerical Methods and Geomechanics, Edmonton, Alberta, Canada, vol. 3, pp. 1137–1152
12. Bažant ZP, Oh BH (1983) Crack band theory for rupture of concrete. Mat Struct (RILEM, Paris) 16: 155–177
13. Bažant ZP, Belytschko TB, Chang T-P (1984) Continuum model for strain softening. J Eng Mech ASCE 110: 1666–1692
14. Bažant ZP (1984) Imbricate continuum and its variational derivation. J Eng Mech ASCE 110: 1693–1712
15. Pijaudier-Cabot G, Bažant ZP (1987) Nonlocal damage theory. J Eng Mech ASCE 113: 1512–1533
16. Bažant ZP, Pijaudier-Cabot G (1988) Nonlocal continuum damage localization instability and convergence. ASME J Appl Mech 55: 287–293
17. Bažant ZP, Lin F-B (1988) Nonlocal smeared cracking model for concrete fracture. J Eng Mech ASCE 114: 2493–2510
18. Bažant ZP, Lin F-B (1988) Nonlocal yield limit degradation. Int J Num Meth Eng 26: 1805–1823
19. Carpinteri A (1994) Fractal nature of material microstructure and size effects on apparent mechanical properties. Mech Mater 18: 89–101
20. Bažant ZP (1997) Scaling of quasibrittle fracture: The fractal hypothesis, its critique and Weibull connection. Int J Fract 83: 41–65
21. Bažant ZP, Yavari, A (2005) Is the cause of size effect on structural strength fractal or energetic-statistical? Eng Fract Mech 72: 1–31
22. Bažant ZP, Yavari A (2007) Response to A. Carpinteri, B. Chiaia, P. Cornetti and S. Puzzi's comments on "Is the cause of size effect on structural strength fractal or energetic-statistical?" Eng Fract Mech 74: 2897–2910
23. Bažant ZP, Daniel IM, Li Z (1996) Size effect and fracture characteristics of composite laminates. ASME Eng Mater Tech 118: 317–324
24. Waddoups ME, Eisenmann JR, Kaminski BE (1971) Microscopic fracture mechanisms of advanced composite materials. J Compos Mater 5: 446–454
25. Cruse TA (1973) Tensile strength of notched composites. J Compos Mater 7: 218–228
26. Mandell JF, Wang S-S, McGarry FJ (1975) The extension of crack tip damage zone in fiber reinforced plastic laminates. J Compos Mater 9: 266–287
27. Whitney JM, Nuismer RJ (1974) Stress fracture criteria for laminated composites containing stress concentrations. J Compos Mater 8: 253–264
28. Daniel IM (1978) Strain and failure analysis of graphite/epoxy plate with cracks. Exp Mech 18: 246–252
29. Daniel IM (1980) Behavior of graphite/epoxy plates with holes under biaxial loading. Exp Mech 20: 1–8
30. Daniel IM (1981) Biaxial testing of graphite/epoxy laminates with cracks. ASTM STP 734 Am Soc Test Mater 734: 109–128
31. Daniel IM (1982) Failure mechanisms and fracture of composite laminates with stress concentrations. In: VIIth International Conference on Experimental Stress Analysis, edited by SEM, Haifa, Israel, Aug. 23–27, pp. 1–20
32. Daniel IM (1985) Mixed-mode failure of composite laminates with cracks. Exp Mech 25: 413–420
33. Bažant ZP (1993) Scaling laws in mechanics of failure. ASCE J Eng Mater 119: 1828–1844
34. Bažant ZP, Zhou Y, Novák D, Daniel IM (2004) Size effect on flexural strength of fiber composite laminates. ASME J Eng Mater Technol 126: 29–37

35. Wisnom MR (1991) The effect of specimen size on the bending strength of unidirectional carbon fiber-epoxy. Compos Struct 18: 47–63
36. Jackson KE (1992) Scaling effects in the flexural response and failure of composite beams. AIAA J 30: 2099–2105
37. Wisnom MR, Atkinson JA (1997) Reduction in tensile and flexural strength of unidirectional glass fiber-epoxy with increasing specimen size. Compos Struct 38: 405–412
38. Johnson DP, Morton J, Kellas S, Jackson KE (2000) Size effect in scaled fiber composites under four-point flexural loading. AIAA J 38: 1047–1054
39. Bažant ZP, Li Z (1995) Modulus of rupture: Size effect due to fracture initiation in boundary layer. ASCE J Struct Eng 121: 739–746
40. Bažant ZP, Novak D (2000) Probabilistic nonlocal theory for quasi-brittle fracture initiation and size effect. I. theory and II. application. ASCE J Eng Mech 126: 166–185
41. Bažant ZP, Novak D (2000) Energetic-statistical size effect in quasi-brittle failure at crack initiation. ACI Mater J 97: 381–392
42. Bažant ZP, Kim J-JH, Daniel IM, Becq-Giraudon E, Zi G (1999) Size effect on compression strength of fiber composites failing by kink band propagation. Int J Fract 95: 103–141
43. Soutis C, Fleck NA, Smith PA (1991) Failure prediction technique for compression loaded carbon fibre-epoxy laminate with open holes. J Compos Mater 25: 1476–1497
44. Budiansky B, Fleck NA, Amazigo JC (1997) On kink-band propagation in fiber composites. J Mech Phys Solid 46: 1637–1653
45. Bažant ZP, Zhou Y, Zi G, Daniel IM (2003) Size effect and asymptotic matching analysis of fracture of closed-cell polymeric foam. Int J Solid Struct 40: 7197–7217
46. Gibson LJ, Ashby MF (1997) Cellular solid-structures and properties (2nd edn.), Cambridge University Press, Cambridge
47. Gdoutos EE, Daniel IM, Wang KA (2002) Failure of cellular foams under multiaxial loading. Compos A 33: 163–176
48. Gdoutos EE, Abot JL (2002) Indentation of cellular foams. In: Gdoutos EE (ed.), Recent Advances in Experimental Mechanics – In Honor of Isaac, M. Daniel, Kluwer, Academic Publishers, Dordrecht, The Netherlands, pp. 55–62
49. Bažant ZP (2005) Scaling of structural strength, 2nd edn., Elsevier, London
50. Bažant ZP, Pfeiffer PA (1987) Determination of fracture energy from size effect and brittleness number. ACI Mater J 84: 463–480
51. Bažant ZP, Kazemi MT (1990) Determination of fracture energy, process zone length and brittleness number from size effect, with application to rock and concrete. Int J Fract 44: 111–131
52. Bažant ZP, Planas J (1998) Fracture and size effect in concrete and other quasibrittle materials, CRC Press, Boca Raton/London (Sections 9.2 and 9.3)
53. Zenkert D, Bäcklund J (1989) PVC sandwich core materials: Mode I fracture toughness. Compos Sci Technol 34: 225–242
54. Bayldon J, Bažant ZP, Daniel IM, Yu Q (2006) Size effect on compressive strength of sandwich panels with fracture of woven laminate facesheet. J Eng Mater Technol 128: 169–174
55. Bažant ZP, Grassl P (2007) Size effect of cohesive delamination fracture triggered by sandwich skin wrinkling. ASME J Appl Mech 74: 1134–1141
56. Bažant ZP (2004) Scaling theory for quasibrittle structural failure. Proc Nat Acad Sci USA 101: 13400–13407